This article was downloaded by: [New York University]
On: 28 May 2015, At: 10:38
Publisher: Taylor & Francis
Informa Ltd Registered in England and Wales Registered Number: 1072954 Registered office: Mortimer House, 37-41 Mortimer Street, London W1T 3JH, UK

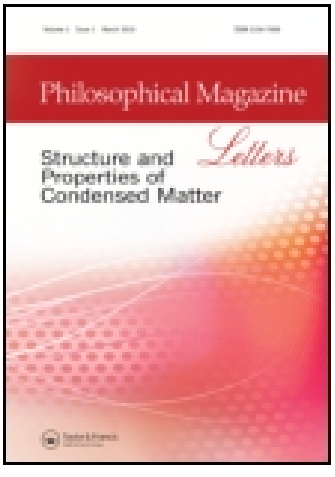

Philosophical Magazine Letters
Publication details, including instructions for authors and subscription information:
http://www.tandfonline.com/loi/tphl20

Nanoscale laser patterning of thin gold films

T. Höche [a c], R. Böhme [a], J. W. Gerlach [a], B. Rauschenbach [a] & F. Syrowatka [b]

[a] Leibniz-Institut für Oberflächenmodifizierung e.V., Permoserstraße 15, D-04318 Leipzig, Germany

[b] Interdisziplinäres Zentrum für Materialwissenschaft, Martin-Luther-Universität Halle-Wittenberg, Hoher Weg 8, D-06120 Halle, Germany

[c] 3D-Micromac AG, Annaberger Straße 240, D-09125 Chemnitz, Germany

Published online: 21 Feb 2007.

To cite this article: T. Höche, R. Böhme, J. W. Gerlach, B. Rauschenbach & F. Syrowatka (2006) Nanoscale laser patterning of thin gold films, Philosophical Magazine Letters, 86:10, 661-667, DOI: 10.1080/09500830600957357

To link to this article: http://dx.doi.org/10.1080/09500830600957357

PLEASE SCROLL DOWN FOR ARTICLE

Taylor & Francis makes every effort to ensure the accuracy of all the information (the "Content") contained in the publications on our platform. However, Taylor & Francis, our agents, and our licensors make no representations or warranties whatsoever as to the accuracy, completeness, or suitability for any purpose of the Content. Any opinions and views expressed in this publication are the opinions and views of the authors, and are not the views of or endorsed by Taylor & Francis. The accuracy of the Content should not be relied upon and should be independently verified with primary sources of information. Taylor and Francis shall not be liable for any losses, actions, claims, proceedings, demands, costs, expenses, damages, and other liabilities whatsoever or howsoever caused arising directly or indirectly in connection with, in relation to or arising out of the use of the Content.

This article may be used for research, teaching, and private study purposes. Any substantial or systematic reproduction, redistribution, reselling, loan, sub-licensing, systematic supply, or distribution in any form to anyone is expressly forbidden. Terms &

Conditions of access and use can be found at http://www.tandfonline.com/page/terms-and-conditions

Downloaded by [New York University] at 10:38 28 May 2015

Philosophical Magazine Letters,
Vol. 86, No. 10, October 2006, 661–667

Taylor & Francis
Taylor & Francis Group

Nanoscale laser patterning of thin gold films

T. HÖCHE*†§, R. BÖHME†, J. W. GERLACH†, B. RAUSCHENBACH†
and F. SYROWATKA‡

†Leibniz-Institut für Oberflächenmodifizierung e.V., Permoserstraße 15,
D-04318 Leipzig, Germany
‡Interdisziplinäres Zentrum für Materialwissenschaft, Martin-Luther-Universität
Halle-Wittenberg, Hoher Weg 8, D-06120 Halle, Germany
§3D-Micromac AG, Annaberger Straße 240, D-09125 Chemnitz, Germany

(*Received 6 June 2006; in final form 3 July 2006*)

Downloaded by [New York University] at 10:38 28 May 2015

Square grids of gold dots were prepared from several nanometer gold films by locally confined excimer laser ablation. Diffraction-mask projection laser ablation at a wavelength of 248 nm was used to convert Au films of 3, 6 and 9 nm thickness on sapphire substrates into well-ordered arrangements of substrate-adhered gold nanodots. Employing a checkerboard phase mask, gold-cap diameters between 75 and 115 nm can be obtained. The methodology allows simultaneous ablation of areas of $\sim 50 \times 50\,\mu m$ in about 1 s and, hence, represents a valuable supplement to the more laborious methods currently in use for the preparation of nanodot template patterns for, say, nanowire growth.

Semiconductor nanowires (NWs) are the subject of intensive investigations due mainly to their unique optical and electrical properties [1]. At present, various approaches to the growth of NWs, including physical and chemical vapour deposition, laser ablation, template-assisted growth or supercritical solution synthesis, have been reported. Popular NW preparation routes, such as vapour–liquid–solid growth and oxide-assisted growth, offer several advantages as these methods enable the preparation of NWs of just a few nanometres diameter and are chemical variable (e.g. heterostructures along the wire axis can be created [2]).

Since the latter two growth techniques make use of nanosized metal dots to take up supersaturated semiconductor vapour on top of the growing nanowire, implementation into devices strictly requires a regular arrangement of those 'seeds' onto the substrate. Therefore, the preparation of regular metal–dot arrays has become a very important issue. In addition to nano-imprint lithography [3] and dip-pen nano-lithography [4], electron lithography [5] and nano-sphere lithography [6, 7] are most frequently applied for this purpose.

In this letter, an alternative, laser-based and very versatile route for the preparation of regularly arranged metal–dot arrays is introduced. This novel

*Corresponding author.

Philosophical Magazine Letters
ISSN 0950-0839 print/ISSN 1362-3036 online © 2006 Taylor & Francis
http://www.tandf.co.uk/journals
DOI: 10.1080/09500830600957357

technique is essentially based on the deposition of a very thin metal film and subsequent application of diffraction-mask projection laser ablation. A similar approach was recently shown to yield nanoscale – yet non-ordered – metal droplets on oxides [8]. Here, we exploit the potential of excimer-laser nanostructuring more fully by imposing a two-dimensional (2D) periodic modulation on the laser intensity distribution. In the one-dimensional case, the capabilities of diffraction-mask projection excimer laser ablation for the fabrication of substrate-adhered nanowires have been demonstrated earlier [9].

The experimental set-up used for diffraction-mask projection laser ablation is shown in figure 1. A checkerboard phase grating, having a period of 11 μm and a depth of ~250 nm, was micromachined into fused-silica (380 μm thickness) by reactive ion-etching (700 eV, 0.2 mA/cm^2, CHF_3) after structuring a resist mask by excimer laser ablation. The grating was specially designed for the existing optical set-up to enhance the ±first-order of diffraction (~60% of the laser output energy is gathered in first order reflections, ~30% remain in the 0th-order and the remaining ~10% enter higher than first-order reflections). The illumination of this mask with a KrF excimer laser (LPX 220i, Lambda Physics; pulse length: 28 ns, repetition rate: 10 Hz, wavelength: 248 nm) results in a spatially modulated laser beam. Utilizing a 36× Schwarzschild-type reflection objective ($NA = 0.5$), the four beams of first-diffraction order imaged onto the sample surface produce an interference pattern over an area of ~50 × 50 μm. Diffracted beams of 0th and higher order were blocked. The 0th-order beam is prevented from reaching the surface, since it is not laterally modulated and would, hence, uniformly illuminate the film to be patterned. It is, therefore, bearing the risk of damaging structures formed on the surface by first diffraction-order beams. Beams of diffraction order higher than one are geometrically also excluded since their direction of propagation is not compatible with the solid angle imaged by the Schwarzschild reflection objective. Their exclusion is beneficial since the intensity of higher-than-first-order beams is too small for

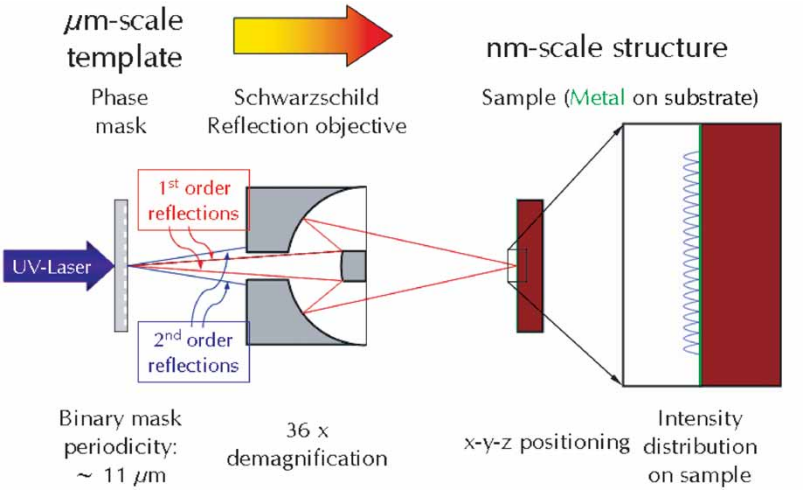

Figure 1. Schematic presentation of the diffraction-mask projection laser-ablation set-up.

Downloaded by [New York University] at 10:38 28 May 2015

effective thin-film ablation. Moreover, the excimer laser used possesses a rather small coherence length. A conventional interference setup with typically long ray paths will be very sensitive with respect to external influences such as mechanical vibrations that disturb the coherence of the beamlets and destroy interference. Hence, rather short distances between the beam-splitting phase mask, imaging objective and sample surface enables the application of low-coherence, multimode laser sources for this special kind of interference technique. In summary, phase-mask projection with a Schwarzschild-type reflection objective is easy to use, versatile and (temporally) stable.

The resulting demagnified and (owing to blocked 0th and > 1st order beams) intrinsically Fourier-filtered image of the mask was used to machine 248-nm transparent, *c*-plane sapphire substrates that were sputter-coated with gold films of three different thicknesses. After deposition, the thickness of the gold films was determined by X-ray reflectometry (XRR) using parallel Cu Kα_1 radiation; values of 3, 6 and 9 nm were obtained. The average laser fluence and pulse numbers were varied in the range of 0.24–1.32 J/cm^2 and 1–100 pulses, respectively. Irradiated areas were imaged in a field-emission environmental scanning electron microscope using 8-keV electrons under a water-vapour pressure of 140 Pa. Gold dots of ~75 nm diameter arranged in a square pattern at a spacing of about 650 nm were found after one-pulse irradiation of the 3-nm thick gold film at a fluence of 1320 mJ/cm^{-2} (figures 2a and 3). In the horizontal direction, the fact that smaller gold droplets occasionally show up is most likely related to the optical alignment (slightly tilted sample with respect to the optical axis and phase-mask imperfections).

Compared to 3-nm thick gold film, the fluence/number of pulses required to ablate the 6-nm film is significantly smaller. This might arise for two reasons. First, the smoothness of the film increases with total film thickness and, second, the laser-specimen interaction is enhanced for thicker gold films. For the 6-nm thick gold film, figure 2b illustrates the gold-dot pattern found after three-pulse irradiation at a fluence of 720 mJ/cm^{-2}. The diameter of individual gold dots has increased to about 110 nm (figure 3) while their spacing remained constant.

Irradiation of the 9-nm thick gold film requires even lower fluences. Already 15 pulses at a fluence of just 400 mJ/cm^{-2} are sufficient to obtain the gold dot arrangement shown in figure 2c. In contrast to the thinner gold films, accumulations of differently sized gold droplets rather than well-separated individual gold dots are found for the 9-nm thick gold film. The latter accumulation would, of course, be detrimental to the growth of well-separated nanowires. From the gold-droplet size distribution plotted in figure 3 (determined from figures 2a–c), it can be further deduced that, while the distribution of gold-dot diameters possesses a bimodal distribution for the 3- and 6-nm thick gold film, the diameter distribution of the gold droplets becomes wider for the 9-nm gold film. Doubling the film thickness from 3 to 6 nm is found to result in a shift of the bimodal distribution towards larger diameters. Contrary to this trend, a further enhancement of film thickness does not lead to droplets of larger size but to the accumulation of a larger number of smaller Au dots.

Upon the excimer-laser nanostructuring reported by Henley *et al.* [8], a contact angle for gold of 120° was found. Considering the side-view micrograph shown in the upper part of figure 2b, it becomes obvious that, in the present case, rather than gold spheres resting on the substrate, shallow spherical gold caps are obtained at positions

Downloaded by [New York University] at 10:38 28 May 2015

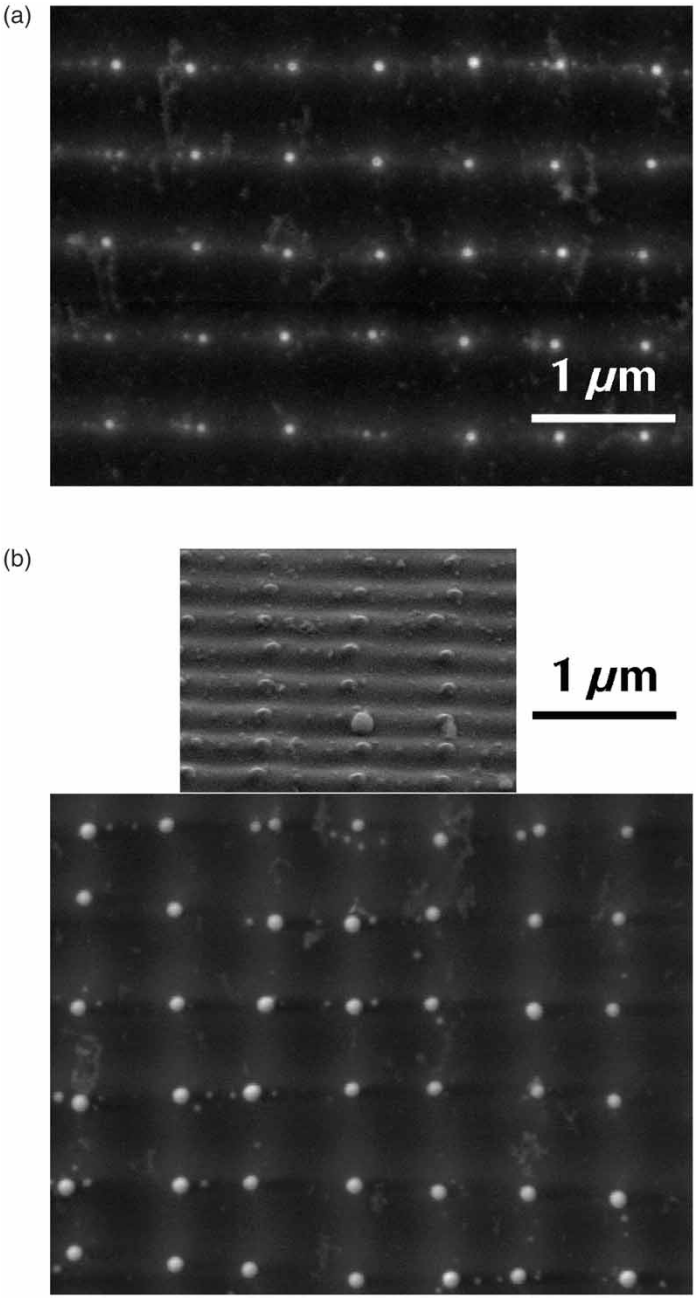

Figure 2. Scanning electron micrographs of gold dot arrangements obtained by: (a) single-pulse irradiation of a 3-nm thick gold film at a fluence of 1320 mJ/cm^{-2}, (b) triple-pulse irradiation of a 6-nm thick gold film at a fluence of 720 mJ/cm^{-2} (above the plan-view micrograph, a side view recorded after tilting the sample by 70° illustrates that the gold dots obtained resemble spherical caps rather than spheres), and (c) 15-pulse irradiation of a 9-nm thick gold film at a fluence of 400 mJ/cm^{-2}.

Downloaded by [New York University] at 10:38 28 May 2015

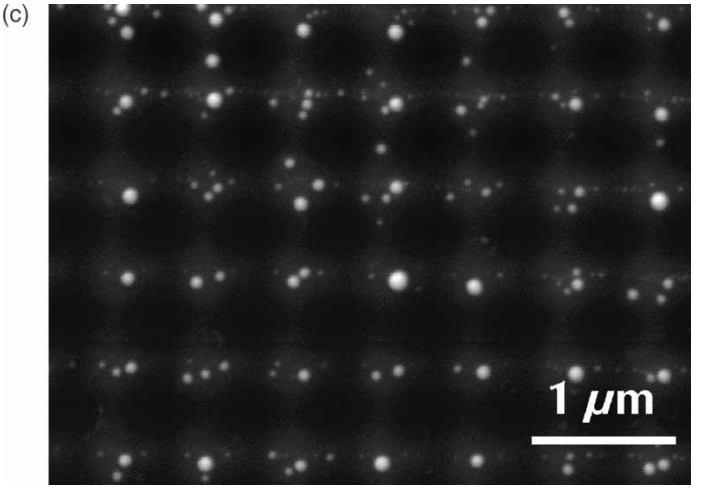

Figure 2. Continued.

Downloaded by [New York University] at 10:38 28 May 2015

where laser-intensity minima are located. The usage of several-times-larger average fluences in comparison to [8] results in a more ablative than annealing regime of interaction between the laser and the gold film. Assuming the cap-like shape of gold dots, the fraction of ablated gold was estimated from figures 2a–c to be around 99% for all three film thicknesses. Occasionally, gold spheres (as the one shown at the top of figure 2b) are observed – but always outside the locations of minimum laser intensity. Hence, such spheres are likely to result from gold clusters condensed in the ablation plume.

From figures 2a–c, it is obvious that the gold-dot diameter cannot simply be adjusted by changing the initial film thickness, as found in recent non-ablating nanostructuring experiments using excimer lasers [8]. While the presently attained size of the gold dots does almost ideally fit the range required for NW growth, smaller dots might be accessible by multi-pulse ablation, as discussed in [9]. To the best of the authors' knowledge, with sufficient stability of laser and mechanics, the preparation of dots with diameters of the order of just a few nanometres should be feasible.

As generally higher laser fluences are required to ablate thinner metal films [8], precise control of the homogeneous film thickness is mandatory to obtain perfect 2D ordering. Given such thickness homogeneity, the arrangement and spacing of resulting gold-dot patterns can be influenced by various parameters. A shorter wavelength (e.g. 157 nm) and a Schwarzschild reflection objective with a larger demagnification factor (objectives up to 74× are commercially available) can be applied to decrease the structural width (distance between neighbouring dots) below 100 nm. The thermal conductivity of the substrate constitutes another important factor that could influence the shape of the gold dots [8]. The presently used sapphire substrate has a relatively large thermal conductivity of about 235 W/m/K. Alternative substrate materials (SiC with a thermal conductivity of 350 W/m/K

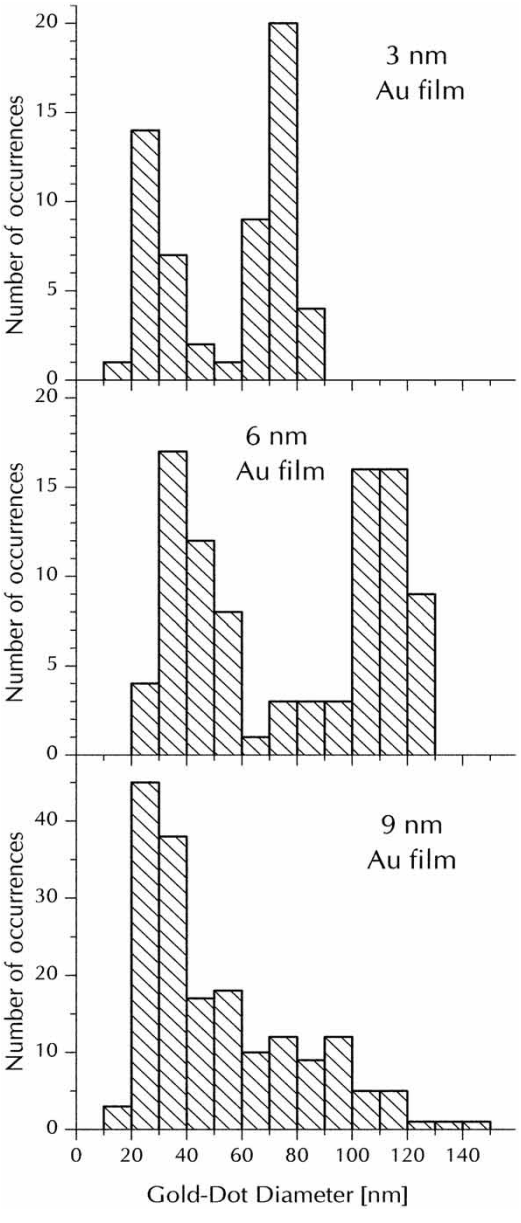

Figure 3. Size distribution of gold dots determined from the scanning electron micrographs shown in figures 2a–c.

or silica glass with 150 W/m/K) are expected to influence the migration behaviour of gold atoms or clusters on the substrate surface.

Beyond the demonstrated square arrangement of dots, more complicated patterns can be generated using, for example, the special interferometric method developed by Simon *et al*. [10], recently applied for the generation of submicron-sized

Downloaded by [New York University] at 10:38 28 May 2015

holes on metal surfaces by femtosecond UV laser pulses. However, in contrast to optical patterning based on many-beam interferences, mask-projection is easier to perform (once a suitable mask is prepared) and the reproducibility of the results is much better. Other modifications of the introduced methodology could include the patterning of other metals, such as nickel and silver.

Acknowledgements

The assistance of U. Gleisberg in the deposition of the gold films is gratefully acknowledged.

Downloaded by [New York University] at 10:38 28 May 2015

References

[1] M.S. Gudiksen, L.J. Lauhon, J. Wang, *et al*., Nature **415** 617 (2002).
[2] H. Pettersson, J. Tragardh, A.I. Persson, *et al*., Nano Lett. **6** 229 (2006).
[3] T. Mårtensson, P. Carlberg, M. Borgström, *et al*., Nano Lett. **4** 699 (2004).
[4] R.D. Piner, J. Zhu, F. Xu, *et al*., Science **283** 661 (1999).
[5] O. Guise, J. Yates, J. Levy, *et al*., Appl. Phys. Lett. **87** 171902 (2005).
[6] K. Kempa, B. Kimball, J. Rybczynski, *et al*., Nano Lett. **3** 13 (2003).
[7] X. Wang, C.J. Summers, Z.L. Wang, *et al*., Nano Lett. **4** 423 (2004).
[8] S.J. Henley, J.D. Carey, S.R.P. Silva, *et al*., Phys. Rev. B **72** 195408 (2005).
[9] T. Höche, R. Böhme, J.W. Gerlach, *et al*., Nano Lett. **4** 895 (2004).
[10] J. Bekesi, J.H. Klein-Wiele, P. Simon, *et al*., Appl. Phys. A Mater. Sci. Process. **76** 355 (2003).